Activation of the thiazide-sensitive Na^+-Cl^- cotransporter by the WNK-regulated kinases SPAK and OSR1

Ciaran Richardson[1,*], Fatema H. Rafiqi[1], Håkan K. R. Karlsson[1], Ntsane Moleleki[1], Alain Vandewalle[2,3], David G. Campbell[1], Nick A. Morrice[1] and Dario R. Alessi[1]

[1]MRC Protein Phosphorylation Unit, MSI/WTB complex, University of Dundee, Dow Street, Dundee, DD1 5EH, UK
[2]INSERM, U773, Centre de Recherche Biomédicale Bichat-Beaujon (CRB3), BP 416, F-75018, Paris, France
[3]Université Paris 7 - Denis Diderot, site Bichat, Paris, F-75870, Paris, France
*Author for correspondence (e-mail: c.j.z.richardson@dundee.ac.uk)

Accepted 30 November 2007
J. Cell Sci. 121, 675-684 Published by The Company of Biologists 2008
doi:10.1242/jcs.025312

Summary

Mutations increasing WNK1 kinase expression in humans cause the pseudohypoaldosteronism type II hypertension syndrome. This condition is treated effectively by thiazide diuretics, which exert their effects by inhibiting the Na^+-Cl^- cotransporter (NCC), suggesting a link between WNK1 and NCC. Here, we demonstrate that the SPAK and OSR1 kinases that are activated by WNK1 phosphorylate human NCC at three conserved residues (Thr46, Thr55 and Thr60). Activation of the WNK1-SPAK/OSR1 signalling pathway by treatment of HEK293 or mpkDCT kidney distal-convoluted-tubule-derived cells with hypotonic low-chloride conditions induced phosphorylation of NCC at residues phosphorylated by SPAK/OSR1. Efficient phosphorylation of NCC was dependent upon a docking interaction between an RFXI motif in NCC and SPAK/OSR1. Mutation of Thr60 to Ala in NCC markedly inhibited phosphorylation of Thr46 and Thr55 as well as NCC activation induced by hypotonic low-chloride treatment of HEK293 cells. Our results establish that the WNK1-SPAK/OSR1 signalling pathway plays a key role in controlling the phosphorylation and activity of NCC. They also suggest a mechanism by which increased WNK1 overexpression could lead to hypertension and that inhibitors of SPAK/OSR1 might be of use in reducing blood pressure by suppressing phosphorylation and hence activity of NCC.

Key words: Cell signalling, Kinase, OSR1, SPAK, WNK1, Cotransporter

Introduction

The STE20/SPS1-related proline/alanine-rich kinase (SPAK, STK39) and oxidative-stress-responsive kinase-1 (OSR1, OXSR1) were discovered through their ability to interact with, phosphorylate and stimulate the activity of the Na^+-K^+-$2Cl^-$ cotransporter (NKCC1, SLC12A2) (Dowd and Forbush, 2003; Piechotta et al., 2003), which plays essential roles in regulating salt/fluid secretion and protecting cells from damage by osmotic stress (reviewed in Flatman, 2007; Gamba, 2005). The SPAK and OSR1 enzymes are phosphorylated and activated by the WNK1 and WNK4 protein kinases (Anselmo et al., 2006; Moriguchi et al., 2005; Vitari et al., 2005), the genes for which are mutated in patients suffering from an inherited hypertension and hyperkalaemia (elevated plasma K^+) disorder, termed pseudohypoaldosteronism type II (Kahle et al., 2007; Wilson et al., 2001).

SPAK and OSR1 consist of an N-terminal catalytic domain belonging to the STE20 kinase subfamily, followed by a conserved region known as the S-motif, and terminate in a unique 92 amino acid sequence sometimes termed the conserved C-terminal (CCT) domain (Vitari et al., 2006). WNK1 activates SPAK and OSR1 by phosphorylating a T-loop residue (Thr233-SPAK, Thr185-OSR1). WNK1 also phosphorylates SPAK and OSR1 at a conserved Ser residue located within the S-motif (Ser373-SPAK, Ser325-OSR1), but the role that this phosphorylation plays is presently unclear, because mutation of this site does not affect activation of SPAK/OSR1 (Vitari et al., 2005; Zagorska et al., 2007). The CCT domain of SPAK/OSR1 functions as a docking site enabling these enzymes to interact with an RFX[I/V]-motif found within their activators (WNK isoforms) as well as their substrates (NKCC1) (Anselmo et al., 2006; Delpire and Gagnon, 2007; Gagnon et al., 2006; Gagnon et al., 2007a; Moriguchi et al., 2005; Piechotta et al., 2003; Vitari et al., 2006). Recently, the structure of the CCT domain of OSR1 complexed to an RFXV-motif-containing peptide derived from WNK4 was reported (Villa et al., 2007). The WNK1 and SPAK/OSR1 kinases are rapidly activated when cells are subjected to hypertonic as well as hypotonic low-chloride conditions (Anselmo et al., 2006; Lenertz et al., 2005; Moriguchi et al., 2005; Zagorska et al., 2007).

The SPAK and OSR1 kinases phosphorylate at least three closely located conserved Thr residues within the N-terminal cytosolic domain of shark NKCC1 that are equivalent to Thr197, Thr201 and Thr206 on mouse NKCC1 (Fig. 1) (Vitari et al., 2006). A recent mutagenesis analysis also demonstrated that mouse NKCC1 was phosphorylated by SPAK at equivalent residues and that mutation of Thr206, but not of Thr197 or Thr201, prevented hyperosmotic-stress-induced activation of mouse NKCC1 expressed in *Xenopus laevis* oocytes (Fig. 1) (Gagnon et al., 2007a). Several other stimuli, including forskolin (activator of PKA) also promote phosphorylation and activation of NKCC1, indicating that multiple signalling pathways control this ion cotransporter (Kurihara et al., 1999; Lytle

Journal of Cell Science

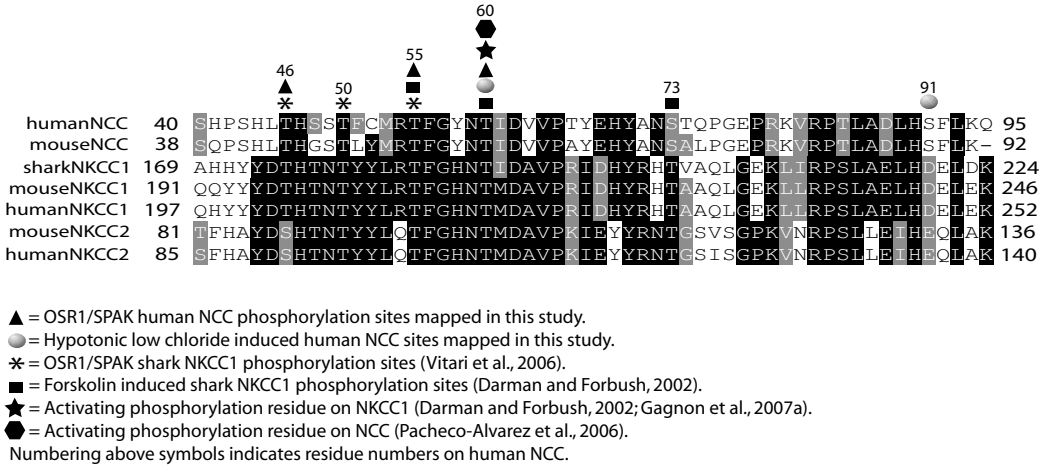

Fig. 1. Sequence alignment of the N-terminal region of SLC12 electroneutral cation-chloride-coupled cotransporters that is regulated by phosphorylation. Identical residues are highlighted in black and similar residues are in grey. Symbols indicate characterised phosphorylation sites.

and Forbush, 3rd, 1992). The phosphorylation sites on NKCC1 induced by forskolin as well as calyculin-A (a phosphatase inhibitor) have been mapped to Thr206 (a SPAK/OSR1 site) as well as to Thr211 and Thr224, which lie C-terminal to the sites phosphorylated by SPAK and OSR1 (Fig. 1) (Darman and Forbush, 2002). The kinases that phosphorylate Thr211 and Thr224 have not been identified. Mutation of the Thr211 residue to Ala abolished activation of NKCC1 by hypotonic low chloride (Darman and Forbush, 2002) as well as by hyperosmotic stress (Gagnon et al., 2007a).

NKCC1 is a member of a superfamily of electroneutral cation-coupled chloride cotransporters (SLC12) that have been subdivided into sodium- and potassium-driven branches (Flatman, 2007; Gamba, 2005). The sodium-driven branch comprises NKCC1 and NKCC2, as well as the Na^+-Cl^- cotransporter (NCC, SLC12A3). The potassium-driven branch comprises four isoforms of the K^+-Cl^- cotransporters (KCC1-KCC4). Sequence alignments indicate that the cluster of phosphorylated Thr residues in NKCC1 is conserved in mouse and human NKCC2 as well as in NCC (Fig. 1). Fragments of these cotransporters containing the cluster of conserved Thr residues are phosphorylated in vitro by the SPAK/OSR1 kinases (Gagnon et al., 2007a; Moriguchi et al., 2005; Vitari et al., 2005; Vitari et al., 2006). The SPAK and OSR1 phosphorylation sites are not conserved in any of the KCC cotransporter isoforms.

Recently, it has been demonstrated that hypotonic low-chloride conditions stimulate the activity and phosphorylation of NCC (Pacheco-Alvarez et al., 2006). Although direct sites of phosphorylation on NCC were not identified in this study, the authors inferred phosphorylation sites by use of a phosphospecific antibody raised against NKCC1 coupled with mutations in NCC to make it recognisable by the NKCC1 phosphospecific antibody. This indicated that hypotonic low-chloride conditions stimulated the phosphorylation of rat NCC at residues Thr53 (equivalent to Thr55 in human NCC and Thr206 in mouse NKCC1) and Thr 58 (equivalent to Thr60 in human NCC and Thr211 in mouse NKCC1) (Pacheco-Alvarez et al., 2006) (Fig. 1). Mutation of Thr58 inhibited activation of rat NCC in a *Xenopus laevis* oocyte heterologous expression system, to a greater extent than mutation of Thr53 (Pacheco-Alvarez et al., 2006).

NCC is primarily expressed in the apical membrane of the mammalian distal convoluted tubule and is the principal regulator of salt transport in this region of the kidney (reviewed in Flatman, 2007; Gamba, 2005). It plays an essential role in regulating extracellular fluid volume and blood pressure. Inactivating mutations in NCC in humans lead to a low-blood-pressure disorder termed Gitelman's syndrome, which also results in renal salt wasting (Flatman, 2007; Gamba, 2005). NCC is also the pharmacological target of the thiazide diuretics that are frequently deployed as the first line of treatment for hypertension (O'Shaughnessy and Karet, 2006). Intriguingly, patients with pseudohypoaldosteronism type II (overexpression of WNK1) are hypersensitive to thiazide diuretic treatment (Wilson et al., 2001; Wilson et al., 2003). This observation, together with the conservation of the SPAK/OSR1 phosphorylation sites, suggests that NCC, like NKCC1, might be phosphorylated and activated by the SPAK/OSR1 pathway. In this study we sought to address this issue. Our data indicate that SPAK and OSR1 interact with NCC and phosphorylate three residues on human NCC (Thr46, Thr55 and Thr60). We demonstrate that endogenously expressed NCC in mpkDCT cells as well as overexpressed NCC in HEK293 cells is phosphorylated at the SPAK/OSR1 targeted residues following activation of the WNK1-SPAK/OSR1 pathway induced by hypotonic low-chloride stress. Our results also indicate that phosphorylation of Thr60 plays the most crucial role in triggering the activation of NCC in HEK293 cells and its mutation also inhibits phosphorylation of the adjacent Thr46 and Thr55 sites. These findings provide novel insights into how NCC is regulated and suggest a mechanism of how WNK1 might regulate blood pressure.

Results

Phosphorylation of NCC by SPAK and OSR1 in vitro

As outlined in the Introduction, several of the reported N-terminal phosphorylation sites on NKCC1 are conserved in NCC, including sites phosphorylated by SPAK and OSR1 (Fig. 1). We therefore tested whether SPAK or OSR1 phosphorylated a fragment of NCC (residues 1-100) encompassing this region of homology with NKCC1 (Fig. 1). NCC[1-100] was readily phosphorylated by active SPAK or OSR1, but not by catalytically inactive mutants of these kinases (Fig. 2A). NCC[1-100] was phosphorylated by OSR1 in a time-dependent manner to a stoichiometry of ~0.1 mol of phosphate/mol of NCC[1-100] (Fig. 2B). [^{32}P]NCC[1-100] phosphorylated by OSR1 was digested with trypsin and chromatographed on a C_{18} column to isolate ^{32}P-labelled phosphopeptides. This revealed four major peaks (P1-P4) (Fig. 2C, upper panel). Mass spectrometry and solid-phase Edman sequencing

Journal of Cell Science

Journal of Cell Science

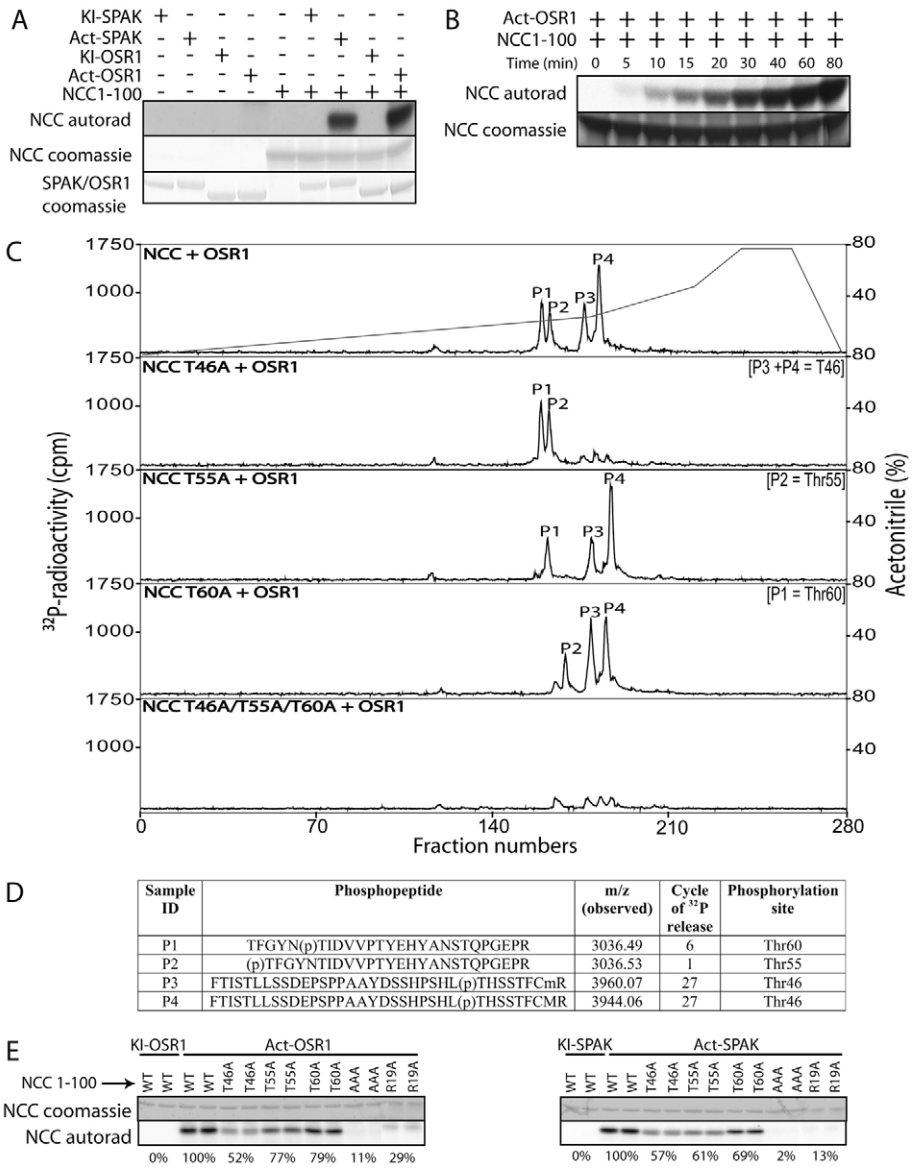

Sample ID	Phosphopeptide	m/z (observed)	Cycle of ^{32}P release	Phosphorylation site
P1	TFGYN(p)TIDVVPTYEHYANSTQPGEPR	3036.49	6	Thr60
P2	(p)TFGYNTIDVVPTYEHYANSTQPGEPR	3036.53	1	Thr55
P3	FTISTLLSSDEPSPPAAYDSSHPSHL(p)THSSTFCmR	3960.07	27	Thr46
P4	FTISTLLSSDEPSPPAAYDSSHPSHL(p)THSSTFCMR	3944.06	27	Thr46

Fig. 2. Identification of residues on NCC that are phosphorylated by OSR1 in vitro. (A) *E. coli*-expressed NCC[1-100] was incubated with the indicated active (Act) and kinase-inactive (KI) forms of OSR1 or SPAK in the presence of Mg-[γ^{32}P]ATP for 40 minutes. Phosphorylation of NCC[1-100] was determined following electrophoresis and subsequent autoradiography of the Colloidal-blue-stained bands corresponding to NCC[1-100]. Similar results were obtained in three separate experiments. KI-SPAK, kinase-inactive SPAK[D212A]; Act-SPAK, activated-SPAK[T233E]; KI-OSR1, kinase-inactive-OSR1[D164A]; Act-OSR1, activated OSR1[T185E]. (B) *E. coli*-expressed NCC[1-100] was incubated with active OSR1 in the presence of Mg-[γ^{32}P]ATP for the indicated times and phosphorylation of NCC[1-100] was determined as in A. (C) The indicated forms of NCC[1-100] were phosphorylated with active OSR1 in the presence of Mg-[γ^{32}P]ATP for 60 minutes. Phosphorylated NCC[1-100] was digested with trypsin and chromatographed on a C_{18} column. The peak fractions containing the major ^{32}P-labelled peptides are labelled P1, P2, P3 and P4. (D) Summary of the mass spectrometry and solid-phase Edman sequencing data obtained following analysis of the indicated phosphopeptides. The deduced amino acid sequence of each peptide is shown and the phosphorylated residue is indicated by (p). 'm' in the peptide sequence indicates methionine sulphoxide. (E) The indicated forms of NCC[1-100] were phosphorylated with kinase-inactive or active OSR1 or SPAK. Phosphorylation was analysed as in A as well as by quantification of ^{32}P radioactivity associated with Colloidal-blue-stained bands corresponding to NCC[1-100]. Results of the latter are presented as a percentage of phosphorylation compared to wild-type (WT) NCC[1-100] by active OSR1/SPAK. Results of duplicate samples are shown and similar results were obtained in two separate experiments. AAA corresponds to a triple NCC[1-100] mutant in which Thr46, Thr55 and Thr60 are changed to Ala.

established the identity of P1 to P4 as diverse tryptic peptides phosphorylated at Thr46, Thr55 and Thr60 (Fig. 2D). This assignment was also confirmed by mutational analysis (Fig. 2C, lower panels). Individual mutation of Thr46, Thr55 and Thr60 decreased overall phosphorylation of NCC[1-100] by OSR1 by 48, 23 and 21%, respectively (Fig. 2E). Mutation of all three residues almost completely inhibited phosphorylation of NCC[1-100] by OSR1. Similar results were observed when NCC[1-100] mutants were phosphorylated by SPAK (Fig. 2E).

Phosphorylation of NCC by SPAK and OSR1 in vivo

To assess whether SPAK and OSR1 might phosphorylate NCC in vivo, we studied phosphorylation of overexpressed human full-length NCC protein in HEK293 cells by mass spectrometry. Cells were treated with either basic control medium or subjected to hypotonic low-chloride medium for 30 minutes in order to activate the WNK1 signalling pathway (Moriguchi et al., 2005). As expected, hypotonic low chloride stimulated the activity as well as the phosphorylation of endogenous WNK1 (Ser382) and SPAK/OSR1 (Thr233/Thr185,) at their T-loop activation residues (Vitari et al., 2005; Zagorska et al., 2007) (Fig. 3A,B). NCC was immunoprecipitated from control and hypotonic low-chloride-treated cells, digested with trypsin and the resulting peptides subjected to phosphopeptide-identification analysis by liquid chromatography-mass spectrometry with precursor ion scanning on a Q-trap mass spectrometer (Fig. 3C). This analysis revealed that hypotonic low-chloride conditions induced phosphorylation of NCC at Thr60 (one of the SPAK/OSR1 sites) as well as at a novel site identified as Ser91. Phosphorylation of a third NCC tryptic peptide, 35 residues in length, containing Thr46 was also observed, but because of the large size of this peptide we were unable to establish which residue was phosphorylated.

To further investigate phosphorylation of NCC, we generated phosphospecific antibodies against the four identified NCC phosphorylation sites (Thr46, Thr55, Thr60 and Ser91). Using these reagents, we corroborate that hypotonic low-chloride treatment of HEK293 cells significantly enhanced the phosphorylation of overexpressed human NCC at these residues (Fig. 4A). The

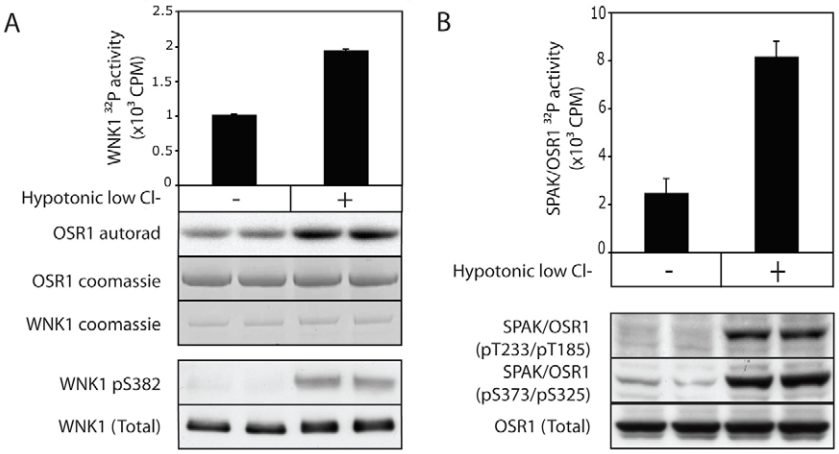

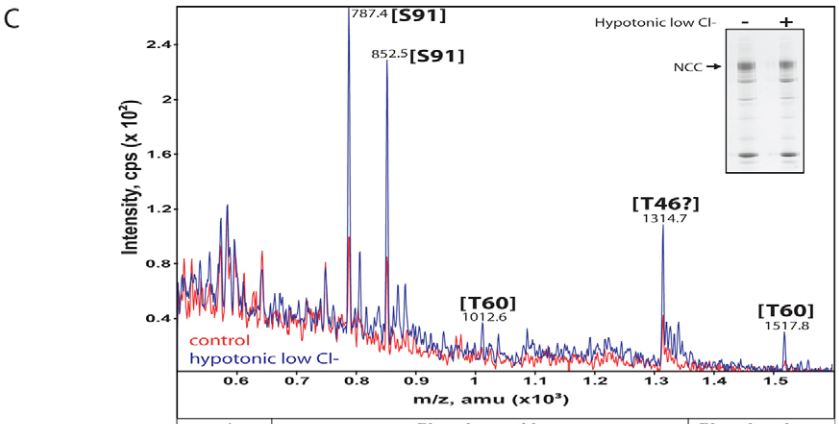

m/z observed	Phosphopeptide	Phosphorylaton site
787.4	VRPTLADLH(p)SFLK	Ser91
852.5	KVRPTLADLH(p)SFLK	Ser91
1012.6	TFGYN(p)TIDVVPTYEHYANSTQPGEPR	Thr60
1314.7	FTISTLLSSDEPSPPAAYDSSHPSHLTHSSTFCMR (+PO_4)	Thr46?
1517.8	TFGYN(p)TIDVVPTYEHYANSTQPGEPR	Thr60

Fig. 3. Characterisation of WNK1-SPAK/OSR1 activity and identification of in vivo phosphorylation sites on NCC. (A) HEK293 cells were treated with either basic (–) or hypotonic low-chloride (+) medium for 30 minutes. Endogenous WNK1 was immunoprecipitated and assayed employing kinase-inactive OSR1 as a substrate. Phosphorylation of OSR1 was determined after electrophoresis followed by autoradiography of the Colloidal-blue-stained bands corresponding to OSR1. The incorporation of ^{32}P radioactivity was also quantified and results are presented as the mean activity ± s.d. for duplicate samples. WNK1 immunoprecipitates were also immunoblotted with the indicated antibodies. (B) As above, except that endogenous SPAK and OSR1 were immunoprecipitated employing an antibody that recognises both proteins. Immunoprecipitated SPAK/OSR1 was assayed employing the CATCHtide peptide substrate (Vitari et al., 2006). Results are presented as the mean activity ± s.d. for duplicate samples. Total cell extracts were also immunoblotted with the indicated antibodies. Results of duplicate samples are shown and similar results were obtained in two separate experiments for A and B. (C) HEK293 cells were transfected with a construct expressing human Flag-NCC. At 36 hours post-transfection, cells were stimulated as in A, and FLAG-NCC was immunoprecipitated and electrophoresed on a polyacrylamide gel. The Colloidal-blue-stained bands corresponding to FLAG-NCC were excised and digested with trypsin. Phosphopeptides were identified by combined liquid chromatography-mass spectrometry and tandem mass spectrometry analysis. The figure shows the signal intensity (cps, counts of ions per second detected) versus the m/z (amu, atomic mass units) for the phosphopeptides derived from NCC isolated from control (red) or hypotonic low-chloride (blue) cells.

specificity of each of the antibodies was verified by demonstrating that mutation of the phosphorylation site to which the antibody was raised against abolished antibody recognition (Fig. 4A). Individual mutation of Thr46, Thr55 or Ser91 to Ala did not markedly affect hypotonic low-chloride-induced phosphorylation of other sites. Strikingly, we observed that mutation of Thr60 to Ala almost completely prevented phosphorylation of Thr46 and Thr55 and inhibited to a lesser extent phosphorylation of Ser91 (Fig. 4A). Performing in vitro phosphorylation experiments, we noted that, in contrast to the experiments performed in cells with full-length NCC, mutation of Thr60 in the NCC[1-100] fragment did not inhibit SPAK and OSR1 from phosphorylating other residues of NCC (Fig. 4B).

We next undertook a time-course analysis of the phosphorylation of NCC in HEK293 cells treated with hypotonic low chloride and in parallel measured phosphorylation of WNK1 and SPAK/OSR1 at their T-loop activation residues (Fig. 4C). WNK1 was rapidly phosphorylated at Ser382, with maximal phosphorylation being observed within 5 minutes and activation sustained for 2 hours. SPAK/OSR1 were activated more slowly, with maximal T-loop phosphorylation being observed at 10 minutes, which was also sustained for 2 hours. Phosphorylation of NCC at the residues phosphorylated by SPAK/OSR1 in vitro (Thr46, Thr55 and Thr60) was detectable at 10 minutes, maximal within 20-30 minutes and sustained for 2 hours. Phosphorylation of NCC at Ser91, a site that is not directly phosphorylated by SPAK/OSR1 in vitro, occurred with similar kinetics to phosphorylation of the SPAK/OSR1 sites (Fig. 4C).

Phosphorylation of NCC is regulated by a docking interaction with SPAK/OSR1

As outlined in the Introduction, the SPAK/OSR1 kinases possess a CCT domain that interacts with RFX[I/V] motifs located within their activators (WNK isoforms) as well as their substrates (NKCC1). Recently, two RFXV motifs located at the N-terminus of NKCC1 were shown to be required for NKCC1 to interact with and be phosphorylated by SPAK (Gagnon et al., 2007a). Inspection of the NCC amino acid sequence revealed that it possesses an optimal CCT-binding RFTI sequence between residues 19 and 22. NCC also possesses another sequence (RFGW, residues 135-138) that could potentially interact with the CCT domain of SPAK/OSR1. In order to investigate whether NCC interacted with SPAK and OSR1 via these motifs, we overexpressed wild-type NCC or mutant NCC, in which Arg19 or Arg135 were mutated to Ala, and verified how this affected binding to SPAK/OSR1. We observed that wild-

Journal of Cell Science

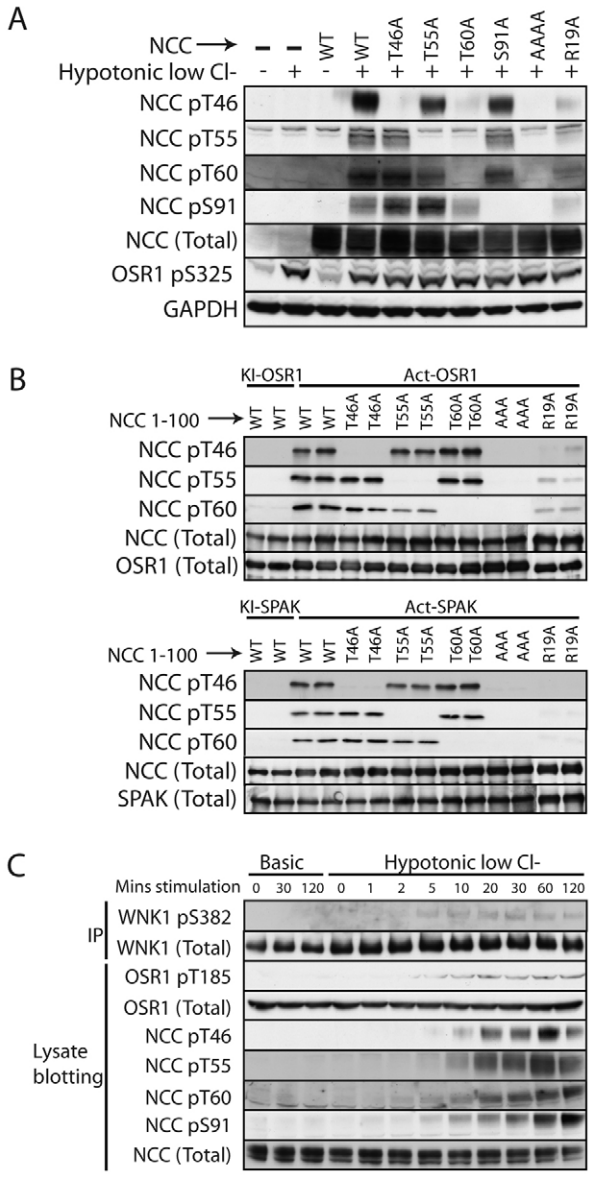

Fig. 4. NCC phosphorylation-site characterisation employing phosphospecific antibodies. (A) HEK293 cells were transfected with wild-type (WT) human FLAG-NCC or the indicated mutant forms of NCC. At 36 hours post-transfection, cells were treated with either basic (–) or hypotonic low-chloride (+) medium for 30 minutes and lysed. Total cell extracts were immunoblotted with NCC-phosphospecific and total antibodies. Similar results were obtained in two separate experiments. AAAA corresponds to a quadruple NCC[1-100] mutant in which Thr46, Thr55, Thr60 and Ser91 are changed to Ala. (B) Wild-type or indicated mutants of NCC[1-100] were phosphorylated with active (Act) or kinase-inactive (KI) mutants of OSR1 or SPAK and phosphorylation analysed by immunoblot analysis. Results of duplicate samples are shown. AAA corresponds to a triple NCC[1-100] mutant in which Thr46, Thr55 and Thr60 are changed to Ala; the kinase-inactive and activated mutants of SPAK/OSR1 employed are defined in the legend to Fig. 2A. (C) HEK293 cells were transfected with wild-type NCC. At 36 hours post-transfection, cells were treated with either basic or hypotonic low-chloride medium for the specified durations and lysed. The phosphorylation of WNK1 at Ser382 and total levels of WNK1 protein were analysed after its immunoprecipitation. Phosphorylation and total levels of SPAK/OSR1 and NCC were analysed in total cell extracts.

type NCC or mutant NCC[R135A] interacted with endogenous SPAK/OSR1, whereas the mutant NCC[R19A] did not bind these

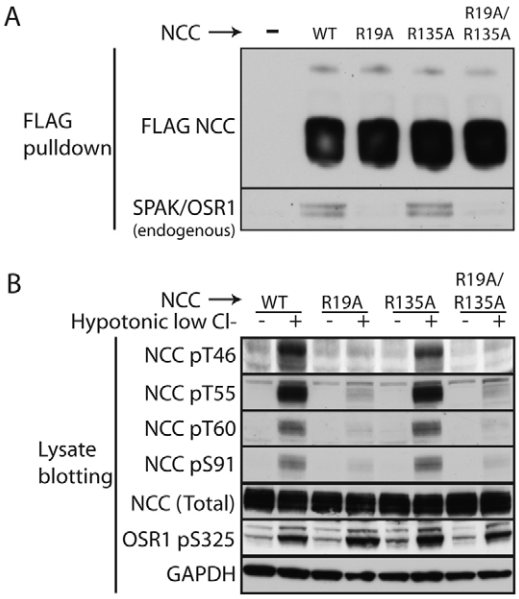

Fig. 5. SPAK/OSR1 interaction with NCC mediates NCC phosphorylation. (A) HEK293 cells were transfected with constructs encoding wild-type (WT) or indicated mutants of human FLAG-NCC. At 36 hours post-transfection, cells were lysed, and NCC was immunoprecipitated and subjected to immunoblot analysis with the indicated antibodies. Similar results were obtained in two separate experiments. (B) As above, except that cells were treated with either basic (–) or hypotonic low-chloride (+) medium for 30 minutes and lysed. Cell lysates were subjected to immunoblot analysis with the indicated antibodies.

kinases (Fig. 5A).

We next investigated how mutation of Arg19 affected phosphorylation of NCC and observed that, following hypotonic low-chloride treatment of cells, mutant NCC[R19A] was poorly phosphorylated at its SPAK/OSR1 sites (Thr46, Thr55 and Thr60). Moreover, phosphorylation of NCC at Ser91, was also markedly reduced in the mutant NCC[R19A] (Fig. 5B). Consistent with Arg135 not mediating interaction with SPAK/OSR1, mutant NCC[R135A] was phosphorylated to a similar extent as the wild-type protein following hypotonic low-chloride treatment of cells (Fig. 5B). Mutation of Arg19 to Ala also markedly inhibited the phosphorylation of NCC by SPAK and OSR1 at all three sites in vitro (Fig. 4B).

Phosphorylation of endogenous NCC in a kidney distal-convoluted-tubule cell line

Expression of the NCC transporter is largely restricted to the distal convoluted tubule of the kidney. Immunoblotting of extracts derived from various cells revealed that the distal-convoluted-tubule-derived cell line termed mpkDCT (Van Huyen et al., 2001) expressed significant levels of endogenous NCC protein (Fig. 6A). NCC was not detected in HEK293 cells or other cell lines that we tested (Fig. 6A). Treatment of mpkDCT cells with hypotonic low-chloride conditions induced significant phosphorylation and activation of the WNK1 and SPAK/OSR1 kinases similar to that observed in HEK293 cells (Fig. 6B,C). Hypotonic low-chloride treatment also markedly stimulated phosphorylation of endogenously expressed NCC in mpkDCT cells at the three residues directly phosphorylated by SPAK/OSR1 (Thr46, Thr55 and Thr60) (Fig. 6D). We were unable to observe phosphorylation of Ser91 in these cells, which

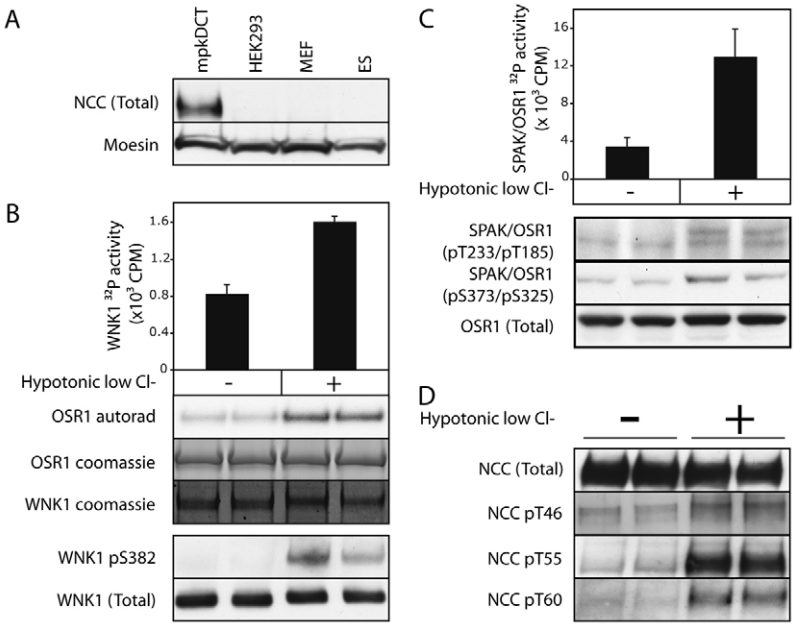

Fig. 6. Endogenous NCC phosphorylation in the mpkDCT cell line. (A) Total cell extracts derived from mpkDCT, HEK293, mouse embryonic fibroblast (MEF) or embryonic stem (ES) cells were immunoblotted with a total NCC antibody from Chemicon (AB3553). Moesin levels were monitored as a loading control. (B,C) mpkDCT cells were treated with either basic (–) or hypotonic low-chloride (+) medium for 30 minutes and lysed. The activity and phosphorylation state of endogenous WNK1 and SPAK/OSR1 were analysed as described in the legend to Fig. 3A,B. Results of duplicate samples are shown and similar results were obtained in two separate experiments. (D) Phosphorylation of endogenous NCC in cell extracts from basic (–) and hypotonic low-chloride (+)-treated mpkDCT cells was determined by immunoblot analysis with the indicated total and phospho-NCC antibodies. Results of duplicate samples are shown and similar results were obtained in two separate experiments.

might be because of sequence variations between the human NCC peptide sequence to which the Ser91 phosphospecific antibody was raised and the corresponding mouse NCC sequence.

Role of identified phosphorylation sites in regulating NCC activity

We next analysed the effect that mutation of the identified phosphorylation sites had on the ability of hypotonic low-chloride conditions to stimulate NCC activation. We expressed full-length human NCC in HEK293 cells that do not express endogenous NCC (Fig. 6A). NCC activity was quantified by measuring thiazide (metolazone)-sensitive radioactive ^{22}Na uptake in control basic medium or hypotonic low-chloride medium. To minimise sodium transport through other channels or cotransporters, cells were treated with ouabain (to inhibit the sodium/potassium ATPase), bumetanide (to inhibit NKCC) and amiloride (to inhibit the ENAC sodium channel) for 15 minutes prior to measuring uptake of radioactive ^{22}Na. In HEK293 cells not transfected with NCC, little thiazide-sensitive ^{22}Na uptake was observed (Fig. 7, panel 1). In cells expressing wild-type NCC, significant thiazide-sensitive ^{22}Na uptake was observed, which was increased ~fourfold following hypotonic low-chloride treatment (Fig. 7, panel 2). Consistent with a previous study undertaken in oocytes (Pacheco-Alvarez et al., 2006), mutation of Thr60 to Ala abolished hypotonic low-chloride-induced activation of NCC (Fig. 7, panel 5). The individual mutation of Thr46, Thr55 or Ser91 had little or no effect on hypotonic-induced activation of NCC (Fig. 7, panels 3, 4 and 6). Consistent with Arg19 of NCC playing a key role in regulating SPAK/OSR1 binding and NCC phosphorylation (Fig. 5), mutant NCC[R19A] was poorly activated by hypotonic low-chloride conditions (Fig. 7, panel 7). Control immunoblotting analysis revealed that NCC mutants employed in this study were expressed at similar levels to the wild-type transporter and were phosphorylated under hypotonic low-chloride conditions employed for these experiments (Fig. 7, lower panels). The results also confirmed our previous observation that mutation of Thr60 to Ala in NCC almost abolished phosphorylation of NCC at Thr46 and Thr55 under hypotonic low-chloride conditions (Fig. 7, lower panel).

Discussion

The data presented in this study demonstrate that SPAK/OSR1 regulate the phosphorylation and activity of human NCC. The residues that SPAK and OSR1 phosphorylate in NCC (Thr46, Thr55 and Thr60) are conserved in all species of NCC that we have analysed and are also conserved in NKCC1 as well as NKCC2, except that, in the latter, the residue equivalent to Thr46 is Ser rather than Thr (Fig. 1). In vitro studies have established that these cotransporters are phosphorylated in vitro by SPAK/OSR1 (Gagnon et al., 2007a; Moriguchi et al., 2005; Vitari et al., 2005; Vitari et al., 2006). The SPAK/OSR1-docking RFX[I/V] motif that we have identified in NCC to be required for efficient phosphorylation by SPAK/OSR1 is also present and plays a similar role in NKCC1 (Gagnon et al., 2007a). NKCC2, which has also been shown to interact with SPAK and OSR1 in a yeast two-hybrid screen (Piechotta et al., 2002), also possesses an N-terminal RFXV motif (residues 20-23 in human NKCC2), suggesting that it will also be phosphorylated and activated by the SPAK and OSR1 kinases. These observations indicate a common mechanism of regulation and activation of the sodium-dependent branch of the SLC12 family of cotransporters. NKCC2 expression is restricted to the apical membrane of renal thick ascending limb cells and is the pharmacological target of the so-called loop diuretics (O'Shaughnessy and Karet, 2006). It is likely that the WNK1-SPAK/OSR1 pathway regulates the phosphorylation and activation of NKCC2 in vivo and it would be interesting to investigate whether this plays a role in regulating blood pressure in mammals.

In a previous study, we identified three SPAK/OSR1 phosphorylation sites on shark NKCC1 that are equivalent to Thr46, Thr50 and Thr55 of human NCC (Vitari et al., 2006). Although we observed phosphorylation of human NCC at Thr46 and Thr55 in the present study, we did not detect phosphorylation of NCC at Thr50 (the residue equivalent to Thr201 in mouse NKCC1; Fig. 1). We also previously failed to observe phosphorylation of the residue

Journal of Cell Science

Journal of Cell Science

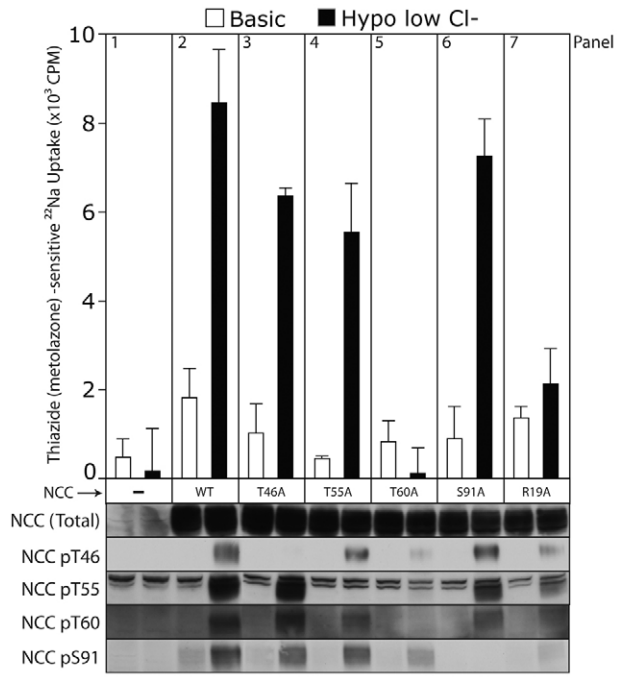

Fig. 7. Mutation of Thr60 of NCC prevents thiazide-sensitive hypotonic low-chloride-induced ^{22}Na uptake in HEK293 cells. HEK293 cells were transfected with pCMV5 empty vector or constructs encoding the indicated wild-type (WT) or mutant forms of human NCC. At 36 hours post-transfection, ^{22}Na uptake was assessed in control basic or hypotonic low-chloride-treated cells in the absence or presence of 0.1 mM metolazone in the uptake medium, as described in the Materials and Methods. For each transfection construct used, metolazone-sensitive ^{22}Na uptake (i.e. metolazone-insensitive counts subtracted) is plotted for both basic and hypotonic low-chloride conditions. The results are presented as the mean ^{22}Na uptake ± s.d. for triplicate samples. Similar results were obtained in three separate experiments. Expression and phosphorylation of NCC proteins were monitored in parallel experiments following immunoblot analysis using the indicated antibodies.

equivalent to Thr60 of human NCC on shark NKCC1 (Vitari et al., 2006). These differences in phosphorylation patterns might result from species and/or conformational and/or amino-acid-sequence differences between NKCC1 and NCC. It is also possible that the bacterially expressed N-terminal fragments of NKCC1 and NCC employed for the in vitro phosphorylation studies are poorly folded and/or phosphorylated at an insufficient stoichiometry at certain residues, inhibiting the identification of these sites by mass spectrometry. Endogenous full-length properly folded and glycosylated NKCC1/NCC cotransporters located within the plasma membrane are likely to be more efficiently phosphorylated than the bacterially expressed fragments of these enzymes. Shark NKCC1 is also phosphorylated in response to forskolin and calyculin-A at Thr189 (equivalent to Thr60 in human NCC and to Thr211 in mouse NKCC1) as well as at Thr184 (equivalent to Thr55 in human NCC and to Thr206 in mouse NKCC1) (Darman and Forbush, 2002). To our knowledge, forskolin or calyculin-A do not stimulate the WNK1 signalling pathway, indicating that distinct kinases might regulate phosphorylation of NKCC1 in response to these agonists.

Our results assessing the activity of wild-type and mutant forms of human NCC in HEK293 cells (Fig. 7) are in agreement with the results obtained by assessing the activity of rat NCC in *Xenopus laevis* oocytes (Pacheco-Alvarez et al., 2006). In both studies, mutation of the residue equivalent to Thr60 in human NCC (Thr58 in rat NCC) severely inhibited activation of NCC by hypotonic low-chloride conditions, whereas mutation of other SPAK/OSR1 phosphorylation sites had few or only moderate effects (Fig. 7). Mutation of the residue equivalent to Thr60 in human NCC in both mouse NKCC1 (Thr211) (Gagnon et al., 2007a) and shark NKCC1 (Thr189) (Darman and Forbush, 2002) also abolished the activation of NKCC1 in response to osmotic stress. These observations point to a vital regulatory function of this residue in controlling the activity of the sodium-driven branch SLC12 cotransporters. Importantly, our data also demonstrate that mutation of Thr60 to Ala markedly inhibited the phosphorylation of NCC at Thr46, Thr55 and to a lesser extent Ser91 (Fig. 4A). Thus, the inhibitory effect of the Thr60-to-Ala mutation on NCC activity might not only result from a loss of Thr60 phosphorylation, but could also result from a loss of phosphorylation of other residues in combination with a loss of Thr60 phosphorylation. It is also possible that the reported inhibitory effects on NKCC1 activity resulting from mutating the residue equivalent to Thr60 (Darman and Forbush, 2002; Gagnon et al., 2007a) could be caused by a loss of phosphorylation of adjacent residues. The mechanism by which the Thr60 mutation in NCC affects phosphorylation of Thr46 and Thr55 is not known. It is possible that phosphorylation of Thr60 primes or induces a conformational change in NCC that promotes phosphorylation of Thr46 and Thr55. This might only arise with full-length NCC, because in vitro studies show that mutation of Thr60 in the NCC[1-100] fragment did not inhibit phosphorylation of Thr46 and Thr55 by SPAK and OSR1 (Fig. 4B). It is also possible that mutation of Thr60 to Ala destabilises NCC in a way that inhibits phosphorylation and/or promotes its dephosphorylation by a protein phosphatase.

We also identified Ser91 on human NCC as a fourth residue whose phosphorylation was enhanced by treatment of cells with hypotonic low chloride. Although Ser91 was not directly phosphorylated by SPAK/OSR1 in vitro (Fig. 2), these enzymes might indirectly regulate the phosphorylation of Ser91 in vivo because mutation of the SPAK/OSR1-RFXI-docking motif on NCC inhibited phosphorylation of Ser91 (Fig. 5B). It is possible that the Ser91 kinase is activated by SPAK/OSR1 or recruited to NCC via SPAK/OSR1, or, alternatively, the Ser91 phosphatase could be inhibited by SPAK/OSR1. We have tested whether WNK1 and the AATYK kinase reported to bind SPAK/OSR1 (Gagnon et al., 2007b) were capable of phosphorylating Ser91, but thus far have not been able to demonstrate direct phosphorylation of NCC at Ser91 by these kinases (C.R., data not shown). We cannot rule out the possibility that, although SPAK/OSR1 does indeed phosphorylate Ser91 in full-length NCC in vivo, it fails to phosphorylate the bacterially expressed NCC[1-100] fragment because this fragment might be mis-folded and/or lack C-terminal docking residues required for SPAK/OSR1 to phosphorylate Ser91. The importance of NCC phosphorylation at Ser91 is also not clear because its mutation to Ala did not affect the activation of NCC by hypotonic low chloride (Fig. 7) or affect phosphorylation of NCC at Thr46, Thr55 or Thr60 (Fig. 4A). Interestingly, the residue equivalent to NCC-Ser91 in NKCC1 or NKCC2 is acidic (Asp-NKCC1 and Glu-NKCC2).

Previous work has suggested that Thr202 in shark NKCC1 (equivalent to Thr224 in mouse NKCC1) is phosphorylated in response to forskolin/calyculin-A treatment (Darman and Forbush, 2002). Mutation of this Thr224 residue in mouse NKCC1 moderately reduces activation following hyperosmotic stress in oocytes by ~20% (Gagnon et al., 2007a). Mutation of the equivalent residue in rat NCC, Ser71 (equivalent to Ser73 in human NCC),

Journal of Cell Science

reduced NCC activation in oocytes following hypotonic low-chloride treatment by ~50% (Pacheco-Alvarez et al., 2006). It has also been reported that, in knock-in mice expressing a pseudohypoaldosteronism mutant form of WNK4[D561], phosphorylation of NCC at this residue is increased (Yang, S. et al., 2007). Our mass spectrometry analysis failed to detect phosphorylation of Ser73 in human NCC following hypotonic low-chloride treatment in cells (Fig. 3C) or following in vitro phosphorylation with OSR1 (Fig. 2). Further work is required to establish whether this is a significant site of phosphorylation and to identify the protein kinases that target this residue and how they might be regulated by WNK isoforms. Without such work it seems premature to use phosphospecific antibodies against Ser73 as a reporter for WNK1-pathway or NCC activity.

A recent investigation based mainly on a series of overexpression experiments suggested that multiple WNK isoforms form a complex that directly regulates NCC (Yang, C. et al., 2007). The precise mechanism by which this complex controls NCC is unclear, but reportedly requires both kinase-independent scaffolding as well as kinase-dependent properties of the different WNK isoforms (Yang, C. et al., 2007). In our opinion, further work is required to establish whether some or all of the effects on NCC activity observed in the Yang et al. study (Yang, C. et al., 2007), as well as other investigations in which wild-type and mutant forms of WNK isoforms were overexpressed in cells, are not meditated via SPAK/OSR1 phosphorylation of NCC. In order to clarify how NCC is regulated by the WNK pathway, we are currently analysing mice that are deficient in SPAK/OSR1 kinase activity as well as in different WNK isoforms. It will be crucial to measure blood pressure as well as the activity and phosphorylation status of NCC and other ion cotransporters in the kidneys of these animals.

In conclusion, our results establish a key role of the WNK1-SPAK/OSR1 signalling pathway in controlling the phosphorylation and activation of NCC. They might provide an explanation as to why overexpression of WNK1 in patients with pseudohypoaldosteronism type II leads to increased blood pressure, by enhancing activity of SPAK/OSR1 and hence phosphorylation and activation of NCC. This would also account for the sensitivity of these patients to treatment with thiazide diuretics that function by inhibiting NCC. Our data also emphasise that inhibitors of SPAK/OSR1 would be expected to reduce NCC phosphorylation and activity, and therefore have the potential to treat hypertension.

Materials and Methods

Materials

Sequencing-grade trypsin (Promega); protease-inhibitor cocktail tablets (Roche); protein-G–Sepharose, glutathione-Sepharose and [γ^{32}P]ATP (Amersham Biosciences); ^{22}Na (PerkinElmer); anti-FLAG M2-agarose, Tween-20, ouabain, bumetanide, amiloride, metolazone, sodium selenite, transferrin, dexamethasone, triiodothyronine, epidermal growth factor, insulin and D-glucose (Sigma-Aldrich); Colloidal blue staining kit and precast SDS polyacrylamide Bis-Tris gels (Invitrogen); Nonidet P40 (Fluka); P81 phosphocellulose paper (Whatman). PreScission protease was expressed and purified from *Escherichia coli* using plasmids kindly provided by John Heath (University of Birmingham, UK). All peptides were synthesised by Graham Bloomberg (University of Bristol School of Medical Sciences, UK).

General methods

Restriction enzyme digests, DNA ligations, other recombinant-DNA procedures, electrophoresis, cell culture and transfections were performed using standard protocols. All mutagenesis was performed using the QuikChange site-directed mutagenesis method (Stratagene) with KOD polymerase (Novagen). DNA constructs used for transfection were purified from *E. coli* DH5α using QIAGEN kits according to the manufacturer's protocol. All DNA constructs were verified by DNA sequencing, which was performed by the Sequencing Service (School of Life Sciences, University of Dundee, UK), using DYEnamic ET terminator chemistry (GE Healthcare) on Applied Biosystems automated DNA sequencers.

Antibodies

The following antibodies were raised in sheep and affinity-purified on the appropriate antigen: NCC phospho-Thr46 antibody [residues 40-54 of human NCC phosphorylated at Thr46, SHPSHL(*P*)THSSTFCMR], NCC phospho-Thr55 antibody [residues 41-60 of human NCC phosphorylated at Thr55, HPSHLTHSSTFCMR(*P*)TFGYNT], NCC phospho-Thr60 antibody [residues 54-66 of human NCC phosphorylated at Thr60, RTFGYN(*P*)TIDVVPT], NCC phospho-Ser91 antibody [residues 85-97 of human NCC phosphorylated at Ser91, TLADLH(*P*)SFLKQEG], WNK1 total antibody (residues 2360-2382 of human WNK1, QNFNISNLQKSISNPPGSNLRTT), WNK1 phospho-Ser382 antibody [residues 377-387 of human WNK1 phosphorylated at Ser382, ASFAK(*P*)SVIGTP], SPAK total antibody (full-length human SPAK protein), OSR1 total antibody (full-length human OSR1 protein), SPAK/OSR1 (T-loop) phospho-Thr233/Thr185 antibody [residues 226-238 of human SPAK or 178-190 of human OSR1, TRNKVRK(*P*)TFVGTP], SPAK/OSR1 (S-motif) phospho-Ser373/Ser325 antibody [residues 367-379 of human SPAK, RRVPGS(*P*)SGHLHKT, which is highly similar to residues 319-331 of human OSR1, in which the sequence is RRVPGS(*P*)SGRLHKT), moesin total antibody (full-length human moesin protein) and GST total antibody (raised against the glutathione S-transferase protein). A commercial total NCC antibody (AB3553) was purchased from Chemicon International. The anti-FLAG antibody (F 1804) was purchased from Sigma-Aldrich and the anti-GAPDH antibody (ab8245) was purchased from Abcam. Secondary antibodies coupled to horseradish peroxidase used for immunoblotting were obtained from Pierce. Pre-immune IgG used in control immunoprecipitation experiments was affinity-purified from pre-immune serum using protein-G–Sepharose.

Buffers

Lysis buffer was 50 mM Tris/HCl, pH 7.5, 1 mM EGTA, 1 mM EDTA, 50 mM sodium fluoride, 5 mM sodium pyrophosphate, 1 mM sodium orthovanadate, 1% (w/v) NP-40, 0.27 M sucrose, 0.1% (v/v) 2-mercaptoethanol and protease inhibitors (1 tablet per 50 ml). Buffer A was 50 mM Tris/HCl, pH 7.5, 0.1 mM EGTA and 0.1% (v/v) 2-mercaptoethanol. TBS-Tween buffer (TTBS) was Tris/HCl, pH 7.5, 0.15 M NaCl and 0.2% (v/v) Tween-20. SDS sample buffer was 1× NuPAGE LDS sample buffer (Invitrogen), containing 1% (v/v) 2-mercaptoethanol. Basic buffer was 135 mM NaCl, 5 mM KCl, 0.5 mM $CaCl_2$, 0.5 mM $MgCl_2$, 0.5 mM Na_2HPO_4, 0.5 mM Na_2SO_4 and 15 mM HEPES. Hypotonic low-chloride buffer was 67.5 mM Na gluconate, 2.5 mM K gluconate, 0.25 mM $CaCl_2$, 0.25 mM $MgCl_2$, 0.5 mM Na_2HPO_4, 0.5 mM Na_2SO_4 and 7.5 mM HEPES.

Plasmids

Cloning of human SPAK and human OSR1 have been described previously (Vitari et al., 2005). Human NCC/SLC12A3 (accession P55017) was amplified employing SuperScript III (Invitrogen) from placenta total RNA (Stratagene) using oligonucleotides GCGGATCCATGGCAGAACTGCCCACAACAGAGA and GCGCGGCCGCTTACTGGCAGTAAAAGGTGAGCACGTTTTC. The RT-PCR product was ligated into pCR2.1-TOPO vector and sequenced. The sequence-verified NCC was sub-cloned into bacterial and mammalian expression vectors using *Bam*HI and *Not*I. Required amino acid mutations were introduced into the pCR2.1-TOPO clone using site-directed mutagenesis by QuikChange method (Stratagene), and sub-cloned into bacterial and mammalian expression vectors.

Cell culture, transfections and stimulations

HEK293 (human embryonic kidney 293) cells were cultured on 10-cm-diameter dishes in DMEM supplemented with 10% (v/v) foetal bovine serum, 2 mM L-glutamine, 100 U/ml penicillin and 0.1 mg/ml streptomycin. The murine distal-convoluted-tubule cell line (mpkDCT) (Van Huyen et al., 2001) was cultured in a defined medium: DMEM:Ham's F12, 1:1 (v/v); 60 nM sodium selenite; 5 μg/ml transferrin; 2 mM L-glutamine; 50 nM dexamethasone; 1 nM triiodothyronine; 10 ng/ml epidermal growth factor (EGF); 5 μg/ml insulin; 20 mM D-glucose; 2% foetal calf serum; and 20 mM HEPES, pH 7.4. For HEK293 transfection experiments, each dish of adherent HEK293 cells was transfected with 20 μl of 1 mg/ml polyethylenimine (Polysciences) and 5-10 μg of plasmid DNA as described previously (Durocher et al., 2002). Transfected HEK293 cells (36 hours post-transfection) or mpkDCT cells were stimulated with either control basic or hypotonic low-chloride medium for periods ranging from 0 to 120 minutes. Cells were lysed in 0.3 ml of ice-cold lysis buffer/dish, lysates were clarified by centrifugation at 4°C for 15 minutes at 26,000 ***g*** and the supernatants were frozen in aliquots in liquid nitrogen and stored at –20°C. Protein concentrations were determined using the Bradford method.

Expression and purification of FLAG-NCC in HEK293 cells

Typically, 10-50 10-cm-diameter dishes of HEK293 cells were cultured and each dish was transfected with 5-10 μg of the pCMV5 construct encoding wild-type or different mutant forms of FLAG-NCC using the polyethylenimine method (Durocher et al., 2002). The cells were cultured for a further 36 hours and lysed in 0.3 ml of ice-cold lysis buffer. The pooled lysate was clarified by centrifugation at 4°C for 15 minutes at 26,000 ***g***. The FLAG-fusion proteins were affinity-purified on FLAG-

Journal of Cell Science

agarose and eluted in either buffer A with 0.1 mg/ml FLAGtide peptide (DYKDDDD) or buffer A containing LDS sample buffer.

Expression and purification of SPAK, OSR1 and NCC[1-100] in *E. coli*

All pGEX-6P-1 constructs were transformed into BL21 *E. coli* cells and 1-litre cultures were grown at 37°C in Luria Broth containing 100 μg/ml ampicillin until the absorbance at 600 nm was 0.8. Isopropyl β-D-thiogalactopyranoside (30 μM) was then added and the cells were cultured for a further 16 hours at 26°C. Cells were isolated by centrifugation, resuspended in 40 ml of ice-cold lysis buffer and lysed in one round of freeze/thawing, followed by sonication (Branson Digital Sonifier; ten 15-second pulses with a setting of 45% amplitude) to fragment DNA. Lysates were centrifuged at 4°C for 15 minutes at 26,000 ***g***. The GST-fusion proteins were affinity-purified on 0.5 ml glutathione-Sepharose and eluted in buffer A containing 0.27 M sucrose and 20 mM glutathione. Alternatively, to cleave GST, the resin was incubated overnight with GST-PreScission protease (50 μg/ 0.5 ml beads).

Immunoblotting

Cell lysates (20-40 μg), purified proteins or immunoprecipitates in SDS sample buffer were subjected to electrophoresis on a polyacrylamide gel and transferred to nitrocellulose membranes. The membranes were incubated for 30 minutes with TTBS containing 10% (w/v) skimmed milk. The membranes were then immunoblotted in 5% (w/v) skimmed milk in TTBS with the indicated primary antibodies overnight at 4°C. Sheep antibodies were used at a concentration of 1-2 μg/ml, whereas commercial antibodies were diluted 1000- to 5000-fold. The incubation with phosphospecific sheep antibodies was performed with the addition of 10 μg/ml of the dephosphopeptide antigen used to raise the antibody. The blots were then washed six times with TTBS and incubated for 1 hour at room temperature with secondary HRP-conjugated antibodies diluted 5000-fold in 5% (w/v) skimmed milk in TTBS. After repeating the washing steps, the signal was detected with the enhanced chemiluminescence reagent. Immunoblots were developed using a film automatic processor (SRX-101; Konica Minolta Medical) and films were scanned with a 300-dpi resolution on a scanner (PowerLook 1000; UMAX). Figures were generated using Photoshop/Illustrator (Adobe).

Immunoprecipitation and assay of WNK1

Anti-WNK1 antibody was coupled with protein-G–Sepharose at a ratio of 1 μg of antibody:1 μl of beads. 1 mg of clarified cell lysate was incubated with 5 μg of anti-WNK1 conjugated to 5 μl of protein-G–Sepharose and incubated for 1 hour at 4°C with gentle agitation. The immunoprecipitates were washed twice with 1 ml of lysis buffer containing 0.5 M NaCl and twice with 1 ml of buffer A. The in vitro phosphorylation reaction mix contained a final volume of 25 μl in buffer A containing 1 μg OSR1[D164A], 0.1 mM [γ^{32}P]ATP and 10 mM $MgCl_2$. The assays were performed for 40 minutes at 30°C and the reaction terminated by adding LDS sample buffer. The samples were electrophoresed on a polyacrylamide gel, which was stained with Colloidal blue, dried and autoradiographed. The OSR1 Coomassie bands were excised and incorporation of ^{32}P radioactivity quantified by Cerenkov counting.

Immunoprecipitation and assay of SPAK and OSR1

1 mg of clarified cell lysate was incubated with 5 μg of the SPAK/OSR1 (total) antibody conjugated to 5 μl of protein-G–Sepharose and incubated for 2 hours at 4°C with gentle agitation. The immunoprecipitates were washed twice with 1 ml of lysis buffer containing 0.5 M NaCl and twice with 1 ml of buffer A. The SPAK/OSR1 immunoprecipitates were assayed with the CATCHtide peptide substrate (RRHYYYDTHTNTYYLRTFGHNTRR), which encompasses the SPAK/OSR1 phosphorylation sites on NKCC1 (Vitari et al., 2006). Assays were set up in a total volume of 50 μl in buffer A containing 10 mM $MgCl_2$, 0.1 mM [γ^{32}P]ATP and 300 μM CATCHtide (RRHYYYDTHTNTYYLRTFGHNTRR). After incubation for 30 minutes at 30°C, the reaction mixture was applied onto P81 phosphocellulose paper, the papers were washed in phosphoric acid and incorporation of ^{32}P radioactivity in CATCHtide was quantified by Cerenkov counting.

Mapping the sites on NCC that are phosphorylated by OSR1

NCC[1-100] (70 μg) purified from *E. coli* was incubated with active OSR1[T185E] (10 μg) also purified from *E. coli* at 30°C for 60 minutes in buffer A containing 10 mM $MgCl_2$, 0.1 mM [γ^{32}P]ATP (approximately 15,000 cpm/pmol) in a total reaction volume of 25 μl. The reaction was terminated by addition of LDS sample buffer. Dithiothreitol (DTT) was added to a final concentration of 10 mM, the samples heated at 95°C for 4 minutes and cooled for 20 minutes at room temperature. Iodoacetamide was then added to a final concentration of 50 mM and the samples left in the dark for 30 minutes at room temperature to alkylate cysteine residues. The samples were subjected to electrophoresis on a Bis-Tris 10% polyacrylamide gel, which was stained with Colloidal blue and then autoradiographed. The phosphorylated NCC[1-100] bands were excised, cut into smaller pieces and washed sequentially for 10 minutes on a vibrating platform with 1 ml of the following: water; 1:1 (v/v) mixture of water and acetonitrile; 0.1 M ammonium bicarbonate; 1:1 mixture of 0.1 M ammonium bicarbonate and acetonitrile; and finally acetonitrile. The gel pieces were dried and incubated for 16 hours at 30°C in 25 mM triethylammonium bicarbonate containing 5 μg/ml trypsin as described previously (Woods et al., 2001). Following tryptic digestion, >95% of the ^{32}P radioactivity incorporated in the gel bands was recovered and the samples were chromatographed on a Vydac 218TP5215 C_{18} column (Separations Group, Hesperia, CA) equilibrated in 0.1% trifluoroacetic acid in water. The column was developed with a linear acetonitrile gradient (diagonal line in Fig. 2C) at a flow rate of 0.2 ml/minute and fractions of 0.1 ml were collected. Some phosphopeptide fractions were further purified by immobilised metal-chelate affinity chromatography on Phos-Select resin (Sigma) as described previously (Beullens et al., 2005).

Phosphopeptide sequence analysis

Isolated phosphopeptides were analysed by MALDI-TOF (matrix-assisted laser-desorption ionisation–time-of-flight)-MS on an Applied Biosystems 4700 Proteomics Analyser using 5 mg/ml α-cyano-4-hydroxycinnamic acid as the matrix. Spectra were acquired in reflector mode and the phosphopeptides were analysed further by performing MALDI-TOF-TOF on selected masses. The characteristic loss of phosphoric acid (molecular mass 98 Da) from the parent phosphopeptide was seen. The site of phosphorylation of all the ^{32}P-labelled peptides was determined by solid-phase Edman degradation on an Applied Biosystems 494C sequencer of the peptide coupled to Sequelon-AA membrane (Applied Biosystems) as described previously (Campbell and Morrice, 2002).

Assay of NCC phosphorylation by SPAK/OSR1

NCC[1-100] and NCC[1-100] mutant proteins (7 μg) purified from *E. coli* were incubated with 1 μg of the following also purified from *E. coli*: kinase-inactive SPAK-SPAK[D212A], active SPAK-SPAK[T233E], kinase-inactive OSR1-OSR1[D164A], or active OSR1-OSR1[T185E]. Reactions were for 40-60 minutes at 30°C in a 25 μl volume in buffer A containing 10 mM $MgCl_2$, 0.1 mM [γ^{32}P]ATP (approximately 1000 cpm/pmol). The reactions were terminated by addition of LDS sample buffer. The samples were electrophoresed on a polyacrylamide gel, which was stained with Coomassie blue, dried and autoradiographed. The NCC[1-100] Coomassie bands were excised and incorporation of ^{32}P radioactivity was quantified by Cerenkov counting.

Identification of phosphorylation sites on FLAG-NCC expressed in HEK293 cells

HEK293 cells were transfected with wild-type FLAG-NCC and, 36 hours post-transfection, cells were treated with either control basic or hypotonic low-chloride medium for 30 minutes. The treated cells were lysed with 0.3 ml of ice-cold lysis buffer/dish and the lysates clarified by centrifugation at 4°C for 15 minutes at 26,000 ***g***. FLAG-NCC was purified from basic or hypotonic low-chloride-treated samples by incubating 30 μl of FLAG-agarose beads with 4 mg of the clarified lysate for 2 hours at 4°C. The immunoprecipitates were washed four times with 1 ml lysis buffer containing 0.5 M NaCl and twice with 1 ml of buffer A. Proteins were eluted from the FLAG beads by the addition of 25 μl 1×NuPAGE LDS sample buffer to the beads. Eluted proteins were reduced by the addition of 10 mM DTT followed by heating at 95°C for 4 minutes. The samples were then alkylated by the addition of 50 mM iodoacetamide followed by incubation in the dark for 30 minutes at room temperature. Samples were then electrophoresed on a 4-12% polyacrylamide gel, which was stained with Colloidal blue. The NCC bands were excised from the gel, cut into smaller pieces and washed as described above. For the identification of phosphorylation sites, the tryptic digests were analysed by LC-MS on an Applied Biosystems 4000 QTRAP system with precursor ion scanning as described previously (Williamson et al., 2006). The resultant MS/MS data were searched using the Mascot search algorithm (www.matrixscience.com) run on a local server.

^{22}Na-uptake assay in HEK293 cells

HEK293 cells were plated at a confluence of 50-60% in 12-well plates (2.4-cm diameter/well) and transfected with wild-type or various mutant forms of full-length human NCC. Each well of HEK293 cells was transfected with 2.5 μl of 1 mg/ml polyethylenimine and 1 μg of plasmid DNA. The ^{22}Na-uptake assay was performed on the cells 36 hours post-transfection. Culture media was removed from the wells and replaced with either basic control or hypotonic low-chloride medium for 15 minutes. Medium was removed and replaced with either basic or hypotonic medium plus inhibitors (1 mM ouabain, 0.1 mM bumetanide, 0.1 mM amiloride) in the presence or absence of 0.1 mM metolazone for a further 15 minutes. After this period, cells were incubated with identical medium containing 2 μCi/ml of ^{22}Na for 85 minutes. After this period, cells were rapidly washed three times with ice-cold non-radioactive medium. The cells were lysed in 300 μl of ice-cold lysis buffer and ^{22}Na uptake quantified on a PerkinElmer liquid scintillation analyser.

We thank the Sequencing Service (School of Life Sciences, University of Dundee, UK) for DNA sequencing, the Post Genomics and Molecular Interactions Centre for Mass Spectrometry facilities (School of Life Sciences, University of Dundee, UK) and the protein-production and antibody-purification teams [Division of Signal Transduction Therapy (DSTT), University of Dundee, UK] co-ordinated

by Hilary McLauchlan and James Hastie for expression and purification of antibodies. We thank the Association for International Cancer Research, Diabetes UK, the Medical Research Council and the pharmaceutical companies supporting the Division of Signal Transduction Therapy Unit (AstraZeneca, Boehringer-Ingelheim, GlaxoSmithKline, Merck & Co., Merck KgaA and Pfizer) for financial support.

References

Anselmo, A. N., Earnest, S., Chen, W., Juang, Y. C., Kim, S. C., Zhao, Y. and Cobb, M. H. (2006). WNK1 and OSR1 regulate the Na^+, K^+, $2Cl^-$ cotransporter in HeLa cells. *Proc. Natl. Acad. Sci. USA* **103**, 10883-10888.

Beullens, M., Vancauwenbergh, S., Morrice, N., Derua, R., Ceulemans, H., Waelkens, E. and Bollen, M. (2005). Substrate specificity and activity regulation of protein kinase MELK. *J. Biol. Chem.* **280**, 40003-40011.

Campbell, D. G. and Morrice, N. A. (2002). Identification of protein phosphorylation sites by a combination of mass spectrometry and solid phase Edman sequencing. *J. Biomol. Tech.* **13**, 121-132.

Darman, R. B. and Forbush, B. (2002). A regulatory locus of phosphorylation in the N terminus of the Na-K-Cl cotransporter, NKCC1. *J. Biol. Chem.* **277**, 37542-37550.

Delpire, E. and Gagnon, K. B. (2007). Genome-wide analysis of SPAK/OSR1 binding motifs. *Physiol. Genomics* **28**, 223-231.

Dowd, B. F. and Forbush, B. (2003). PASK (proline-alanine-rich STE20-related kinase), a regulatory kinase of the Na-K-Cl cotransporter (NKCC1). *J. Biol. Chem.* **278**, 27347-27353.

Durocher, Y., Perret, S. and Kamen, A. (2002). High-level and high-throughput recombinant protein production by transient transfection of suspension-growing human 293-EBNA1 cells. *Nucleic Acids Res.* **30**, E9.

Flatman, P. W. (2007). Cotransporters, WNKs and hypertension: important leads from the study of monogenetic disorders of blood pressure regulation. *Clin. Sci. Lond.* **112**, 203-216.

Gagnon, K. B., England, R. and Delpire, E. (2006). Volume sensitivity of cation-Cl- cotransporters is modulated by the interaction of two kinases: Ste20-related proline-alanine-rich kinase and WNK4. *Am. J. Physiol. Cell Physiol.* **290**, C134-C142.

Gagnon, K. B., England, R. and Delpire, E. (2007a). A single binding motif is required for SPAK activation of the Na-K-2Cl cotransporter. *Cell. Physiol. Biochem.* **20**, 131-142.

Gagnon, K. B., England, R., Diehl, L. and Delpire, E. (2007b). Apoptosis-associated tyrosine kinase scaffolding of protein phosphatase 1 and SPAK reveals a novel pathway for Na-K-2C1 cotransporter regulation. *Am. J. Physiol. Cell Physiol.* **292**, C1809-C1815.

Gamba, G. (2005). Molecular physiology and pathophysiology of electroneutral cation-chloride cotransporters. *Physiol. Rev.* **85**, 423-493.

Kahle, K. T., Ring, A. M. and Lifton, R. P. (2007). Molecular physiology of the WNK kinases. *Annu. Rev. Physiol.* doi: 10.1146/annurev.physiol.70.113006.100651.

Kurihara, K., Moore-Hoon, M. L., Saitoh, M. and Turner, R. J. (1999). Characterization of a phosphorylation event resulting in upregulation of the salivary Na(+)-K(+)-2Cl(–) cotransporter. *Am. J. Physiol.* **277**, C1184-C1193.

Lenertz, L. Y., Lee, B. H., Min, X., Xu, B. E., Wedin, K., Earnest, S., Goldsmith, E. J. and Cobb, M. H. (2005). Properties of WNK1 and implications for other family members. *J. Biol. Chem.* **280**, 26653-26658.

Lytle, C. and Forbush, B., 3rd (1992). The Na-K-Cl cotransport protein of shark rectal gland. II. Regulation by direct phosphorylation. *J. Biol. Chem.* **267**, 25438-25443.

Moriguchi, T., Urushiyama, S., Hisamoto, N., Iemura, S., Uchida, S., Natsume, T., Matsumoto, K. and Shibuya, H. (2005). WNK1 regulates phosphorylation of cation-chloride-coupled cotransporters via the STE20-related kinases, SPAK and OSR1. *J. Biol. Chem.* **280**, 42685-42693.

O'Shaughnessy, K. M. and Karet, F. E. (2006). Salt handling and hypertension. *Annu. Rev. Nutr.* **26**, 343-365.

Pacheco-Alvarez, D., Cristobal, P. S., Meade, P., Moreno, E., Vazquez, N., Munoz, E., Diaz, A., Juarez, M. E., Gimenez, I. and Gamba, G. (2006). The Na+:Cl- cotransporter is activated and phosphorylated at the amino-terminal domain upon intracellular chloride depletion. *J. Biol. Chem.* **281**, 28755-28763.

Piechotta, K., Lu, J. and Delpire, E. (2002). Cation chloride cotransporters interact with the stress-related kinases Ste20-related proline-alanine-rich kinase (SPAK) and oxidative stress response 1 (OSR1). *J. Biol. Chem.* **277**, 50812-50819.

Piechotta, K., Garbarini, N., England, R. and Delpire, E. (2003). Characterization of the interaction of the stress kinase SPAK with the Na^+-K^+-$2Cl^-$ cotransporter in the nervous system: evidence for a scaffolding role of the kinase. *J. Biol. Chem.* **278**, 52848-52856.

Van Huyen, J. P., Bens, M., Teulon, J. and Vandewalle, A. (2001). Vasopressin-stimulated chloride transport in transimmortalized mouse cell lines derived from the distal convoluted tubule and cortical and inner medullary collecting ducts. *Nephrol. Dial. Transplant.* **16**, 238-245.

Villa, F., Goebel, J., Rafiqi, F. H., Deak, M., Thastrup, J., Alessi, D. R. and van Aalten, D. M. (2007). Structural insights into the recognition of substrates and activators by the OSR1 kinase. *EMBO Rep.* **8**, 839-845.

Vitari, A. C., Deak, M., Morrice, N. A. and Alessi, D. R. (2005). The WNK1 and WNK4 protein kinases that are mutated in Gordon's hypertension syndrome phosphorylate and activate SPAK and OSR1 protein kinases. *Biochem. J.* **391**, 17-24.

Vitari, A. C., Thastrup, J., Rafiqi, F. H., Deak, M., Morrice, N. A., Karlsson, H. K. and Alessi, D. R. (2006). Functional interactions of the SPAK/OSR1 kinases with their upstream activator WNK1 and downstream substrate NKCC1. *Biochem. J.* **397**, 223-231.

Williamson, B. L., Marchese, J. and Morrice, N. A. (2006). Automated identification and quantification of protein phosphorylation sites by LC/MS on a hybrid triple quadrupole linear ion trap mass spectrometer. *Mol. Cell. Proteomics* **5**, 337-346.

Wilson, F. H., Disse-Nicodeme, S., Choate, K. A., Ishikawa, K., Nelson-Williams, C., Desitter, I., Gunel, M., Milford, D. V., Lipkin, G. W., Achard, J. M. et al. (2001). Human hypertension caused by mutations in WNK kinases. *Science* **293**, 1107-1112.

Wilson, F. H., Kahle, K. T., Sabath, E., Lalioti, M. D., Rapson, A. K., Hoover, R. S., Hebert, S. C., Gamba, G. and Lifton, R. P. (2003). Molecular pathogenesis of inherited hypertension with hyperkalemia: the Na-Cl cotransporter is inhibited by wild-type but not mutant WNK4. *Proc. Natl. Acad. Sci. USA* **100**, 680-684.

Woods, Y. L., Rena, G., Morrice, N., Barthel, A., Becker, W., Guo, S., Unterman, T. G. and Cohen, P. (2001). The kinase DYRK1A phosphorylates the transcription factor FKHR at Ser329 in vitro, a novel in vivo phosphorylation site. *Biochem. J.* **355**, 597-607.

Yang, C. L., Zhu, X. and Ellison, D. H. (2007). The thiazide-sensitive Na-Cl cotransporter is regulated by a WNK kinase signaling complex. *J. Clin. Invest.* **117**, 3403-3411.

Yang, S. S., Morimoto, T., Rai, T., Chiga, M., Sohara, E., Ohno, M., Uchida, K., Lin, S. H., Moriguchi, T., Shibuya, H. et al. (2007). Molecular pathogenesis of pseudohypoaldosteronism type II: generation and analysis of a Wnk4(D561A/+) knockin mouse model. *Cell Metab.* **5**, 331-344.

Zagorska, A., Pozo-Guisado, E., Boudeau, J., Vitari, A. C., Rafiqi, F. H., Thastrup, J., Deak, M., Campbell, D. G., Morrice, N. A., Prescott, A. R. et al. (2007). Regulation of activity and localization of the WNK1 protein kinase by hyperosmotic stress. *J. Cell Biol.* **176**, 89-100.

Journal of Cell Science